MUC1-C promotes the suppressive immune microenvironment in non-small cell lung cancer

Audrey Bouillez, Dennis Adeegbe, Caining Jin, Xiufeng Hu, Ashujit Tagde, Maroof Alam, Hasan Rajabi, Kwok-Kin Wong & Donald Kufe

View supplementary material 🗗

Accepted author version posted online: 05 Jul 2017.
Published online: 14 Aug 2017.

Submit your article to this journal 🗗

Article views: 271

View Crossmark data 🗗

Citing articles: 3 View citing articles 🗗

Taylor & Francis
Taylor & Francis Group

BRIEF REPORT

Check for updates

MUC1-C promotes the suppressive immune microenvironment in non-small cell lung cancer

Audrey Bouillez*, Dennis Adeegbe*, Caining Jin, Xiufeng Hu, Ashujit Tagde, Maroof Alam, Hasan Rajabi, Kwok-Kin Wong**, and Donald Kufe

Dana-Farber Cancer Institute, Harvard Medical School, Boston, MA, USA

ABSTRACT

The cancer immune microenvironment is of importance for the effectiveness of immunotherapy; however, its dysregulation is poorly understood. The MUC1-C oncoprotein is aberrantly overexpressed in non-small cell lung cancer (NSCLC) and has been linked to the induction of PD-L1. The present work investigated the effects of targeting MUC1-C in an immuno-competent MUC1 transgenic (MUC1.Tg) mouse model. We show that Lewis Lung Carcinoma cells expressing MUC1-C (LLC/MUC1) exhibit upregulation of PD-L1 and suppression of interferon-γ (IFN-γ). In studies of LLC/MUC1 cells growing *in vitro* and as tumors in MUC1.Tg mice, treatment with the MUC1-C inhibitor, GO-203, was associated with the downregulation of PD-L1 and induction of IFN-γ. The results further demonstrate that targeting MUC1-C results in enhanced effector function of CD8+ tumor-infiltrating lymphocytes (TILs) as evidenced by increased expression of the activation marker CD69, the degranulation marker CD107α, and granzyme B. Notably, targeting MUC1-C was also associated with marked increases in TIL-mediated killing of LLC/MUC1 cells. Analysis of gene expression data sets further showed that overexpression of *MUC1* in NSCLCs correlates negatively with *CD8, IFNG* and *GZMB*, and that decreases in *CD8* and *IFNG* are associated with poor clinical outcomes. These findings in LLC/MUC1 tumors and in NSCLCs indicate that MUC1-C→PD-L1 signaling promotes the suppression of CD8+ T-cell activation and that MUC1-C is a potential target for reprogramming of the tumor microenvironment.

Abbreviations: EMT, epithelial-mesenchymal transition; LLC, Lewis Lung Carcinoma; LLC/MUC1, MUC1-expressing LLC; MUC1, mucin 1; MUC1-C, MUC1 C-terminal subunit; NSCLC, non-small cell lung cancer; PD-L1, programmed death ligand 1; PD-1, programmed death 1; TILs, tumor-infiltrating lymphocytes

Introduction

Immunotherapy has markedly changed the landscape of non-small cell lung cancer (NSCLC) treatment. Targeting the programmed death 1/programmed death ligand 1 (PD-1/PD-L1) immune checkpoint has improved response rates and overall survival for NSCLC patients compared with that achieved with chemotherapy.[1-5] Notably, however, PD-1/PD-L1 blockade has been limited by response rates of ~20–30% and, in certain NSCLC patients, a limited duration of response.[6] Studies of NSCLCs have also shown that the density of CD8+ tumor-infiltrating lymphocytes (TILs) is positively associated with survival,[7-9] further supporting the premise that immune evasion contributes to the pathogenesis of this disease. Significantly, few mechanistic insights are available regarding how NSCLCs evade immune recognition and destruction. In this regard, the present study evaluated how mucin 1 (MUC1) expression in tumor cells contributes to evasion of immune recognition and destruction in a model of NSCLC. MUC1 is a heterodimeric glycoprotein which is aberrantly overexpressed in >80% of NSCLCs and is associated with poor clinical outcomes.[10-12] The

MUC1 C-terminal (MUC1-C) oncogenic subunit directly activates the TAK1→IKK→NF-κB p65 pathway in cancer cells and integrates this inflammatory response with induction of the epithelial-mesenchymal transition (EMT), stemness and self-renewal capacity.[13] In addition, MUC1-C-mediated activation of the NF-κB p65 pathway has been linked to the induction of PD-L1 expression in *in vitro* studies of human NSCLC cells.[14] The present studies have extended this observation by uncovering a previously unrecognized role for MUC1-C in programming the NSCLC immune microenvironment and thereby emphasize the importance of MUC1-C as a target for the immunotherapy of this disease.

Results and discussion

Evidence is accumulating that MUC1-C plays a role in the regulation of genes, such as *PD-L1*, that promote the evasion of NSCLC cells from immune recognition.[14] However, there is no available evidence that MUC1-C has any functional role in immune evasion in tumor models or in patients. Accordingly, we studied Lewis Lung Carcinoma

---

(LLC) cells stably expressing human MUC1 (LLC/MUC1). As expected, LLC/MUC1 cells exhibited high levels of MUC1 mRNA relative to that in control LLC cells expressing an empty vector (LLC/vector) (Fig. 1A). We also found that MUC1 increases PD-L1 and suppresses IFN-γ mRNA levels (Fig. 1A). MUC1 is a heterodimeric complex consisting of an extracellular N-terminal subunit (MUC1-N) and a transmembrane C-terminal subunit (MUC1-C) that functions as an oncoprotein.[13,15,16] MUC1-C (20–25 kDa) includes a short extracellular domain, a transmembrane domain and an intrinsically disordered 72 amino acid cytoplasmic domain, which interacts with diverse kinases and effectors, such as NF-κB p65, that have been linked to inflammation and transformation (Fig. S1).[13,15,16] In this context, MUC1 expression in LLC/MUC1 cells was associated with upregulation of PD-L1 protein (Fig. 1B). Additionally, overexpression of human MUC1-C in LLC cells was associated with induction of PD-L1 and suppression of IFN-γ (Fig. 1C), indicating that MUC1-C and not MUC1-N is sufficient for these responses. The MUC1-C cytoplasmic
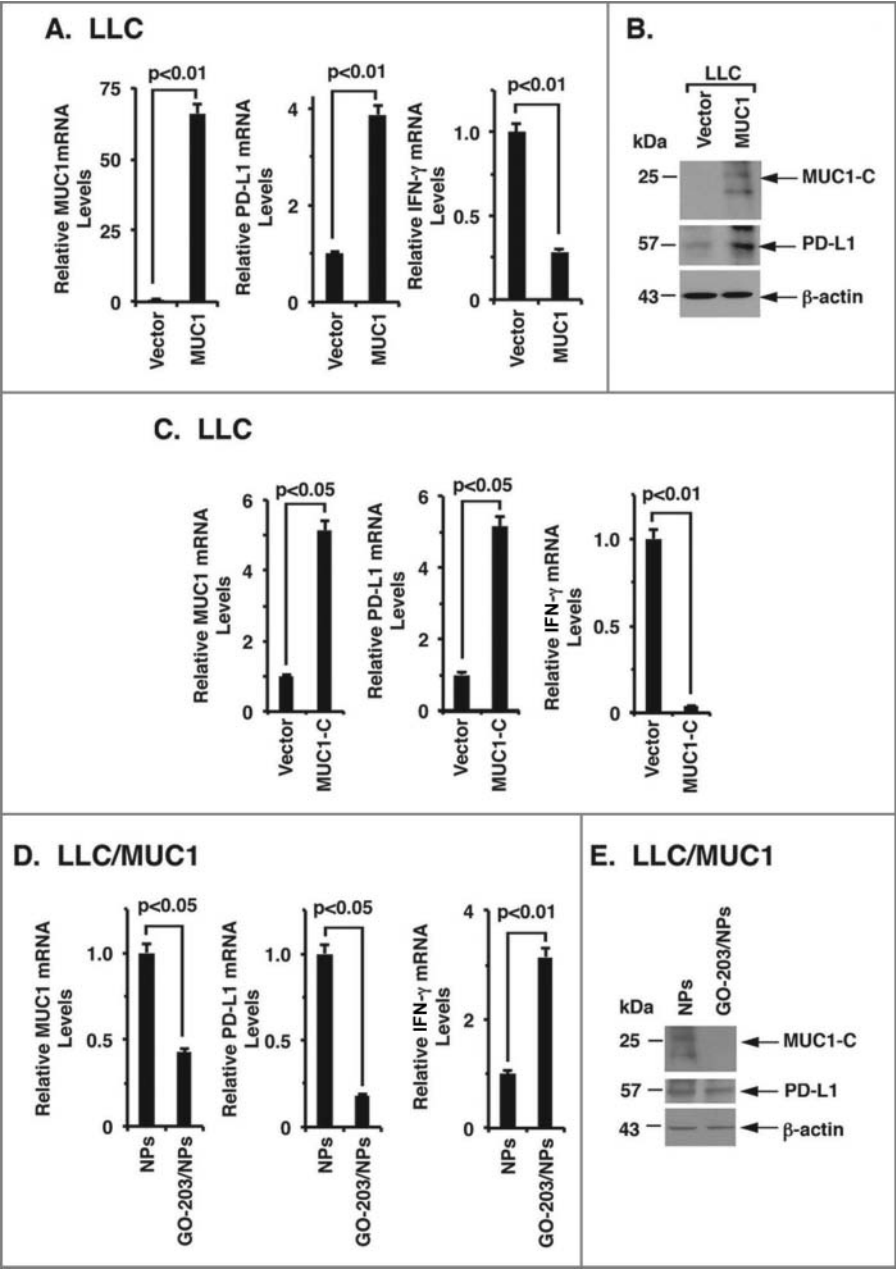

Figure 1. MUC1-C regulates PD-L1 and IFN-γ expression in LLC NSCLC cells. (A) Lewis Lung Carcinoma (LLC) NSCLC cells stably expressing a control empty vector (LLC/Vector) or full length MUC1 (LLC/MUC1) were analyzed for MUC1, PD-L1 and IFN-γ mRNA levels by qRT-PCR. The results (mean $\pm$ SEM of 3 biologic replicates each performed in triplicate) are expressed as relative mRNA levels as compared with that obtained for the vector cells (assigned a value of 1). (B) Lysates from LLC/Vector and LLC/MUC1 cells were immunoblotted with the indicated antibodies. (C) LLC cells expressing a control empty vector (LLC/Vector) or MUC1-C (LLC/MUC1-C) were analyzed for MUC1, PD-L1 and IFN-γ mRNA levels by qRT-PCR. The results (mean $\pm$ SEM of 3 biologic replicates each performed in triplicate) are expressed as relative mRNA levels as compared with that obtained for the vector cells (assigned a value of 1). (D) LLC/MUC1 cells were treated with empty NPs or 2.5 μM GO-203/NPs for 72 h. Cells were analyzed for MUC1, PD-L1 and IFN-γ mRNA levels by qRT-PCR. The results (mean $\pm$ SEM of 3 biologic replicates each performed in triplicate) are expressed as relative mRNA levels as compared with that obtained for the NP-treated cells (assigned a value of 1). (E) Lysates from the designated LLC/MUC1 cells were immunoblotted with the indicated antibodies.
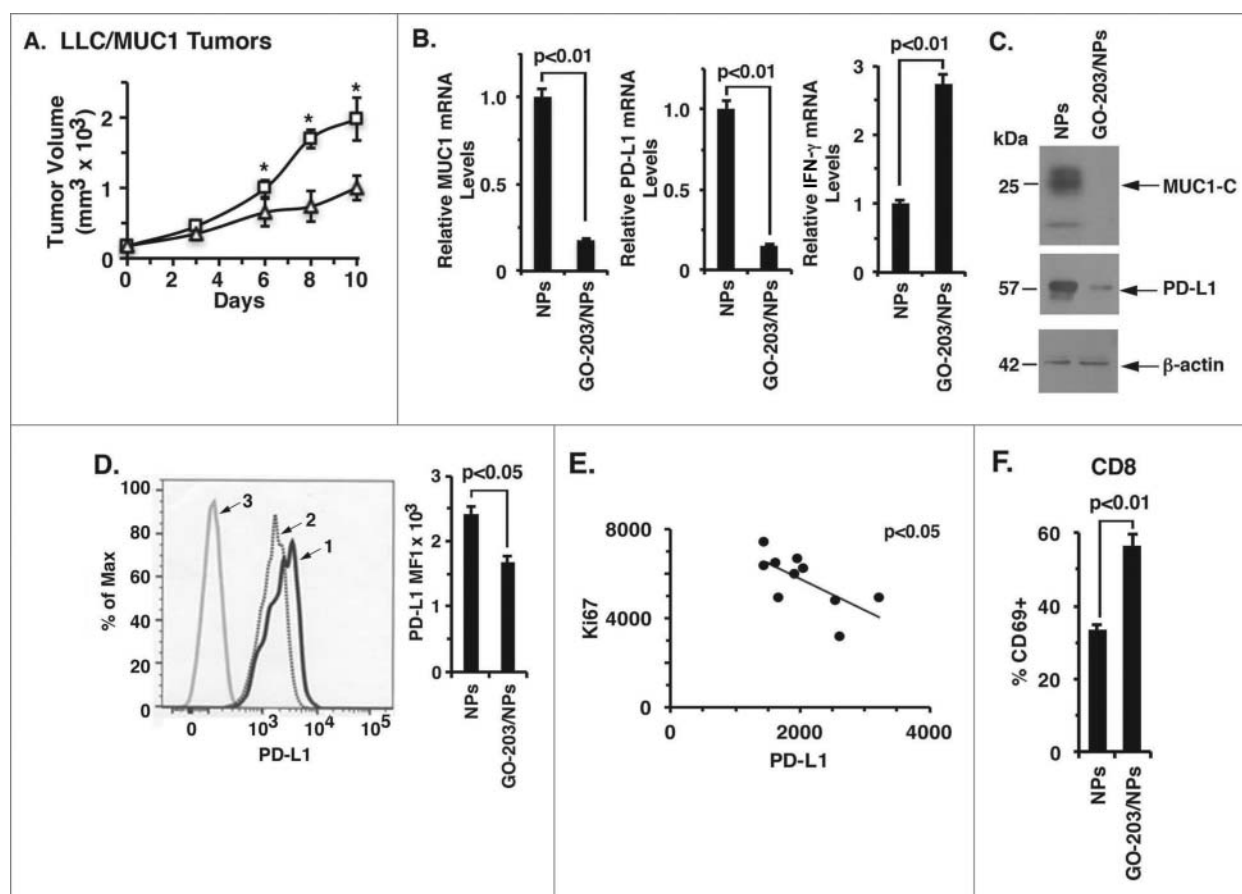
Figure 2. Targeting MUC1-C activates the LLC tumor immune microenvironment in a MUC1.Tg mouse model. (A) Mice bearing established LLC/MUC1 tumor xenografts (~150 mm³) were treated weekly with intraperitoneal injections of empty NPs (squares) or 15 mg/kg GO-203/NPs (triangles). The results are expressed as tumor volume (mean ± SEM, 6 mice per group). * denotes $p < 0.05$. (B) Tumors harvested from empty NP- and GO-203/NP-treated mice (day 10) were analyzed for MUC1, PD-L1 and IFN-γ mRNA levels by qRT-PCR. The results (mean ± SEM of 3 biologic replicates each performed in triplicate) are expressed as relative mRNA levels as compared with that obtained for the control NP-treated mice (assigned a value of 1). (C) Tumors obtained on day 10 were immunoblotted with the indicated antibodies. (D-F) Single cell suspensions were generated from the LLC/MUC1 tumor tissues and subjected to FACS analysis. (D) In a representative histogram, tumor cells from NP-treated (profile #1) and GO-203/NP-treated (profile #2) mice were analyzed for PD-L1 expression (left). An isotype identical antibody was used as an internal control (profile #3) (left). The percentage of PD-L1-positive tumor cells is expressed as the mean ± SEM for 5 tumors per group(right). (E) Expression levels of Ki67 on T-cells relative to PD-L1 on tumor cells. (F) Tumor-infiltrating CD8+ cells were analyzed for CD69 expression. The results are expressed as the percentage (mean ± SEM for 5 tumors per group) of CD69 positive cells.

domain contains a CQC motif that is necessary for MUC1-C homodimerization and thereby functions in signaling at the cell membrane and in the nucleus (Fig. S1).[13,15,16] Accordingly, we developed the GO-203 peptide inhibitor, which includes a poly-R transduction domain linked to CQCRRKN, to target the CQC motif and block MUC1-C homodimerization and function (Fig. S1).[17,18] GO-203 has also been formulated in polymeric nanoparticles (GO-203/NPs) for sustained delivery in mouse tumor models.[19] In concert with these and the above findings, treatment of LLC/MUC1 cells with GO-203/NPs, but not empty NPs, was associated with the (i) downregulation of MUC1-C and PD-L1, and (ii) induction of IFN-γ expression (Fig. 1D and E).

To extend this line of investigation, we performed studies in an immune competent MUC1 transgenic (MUC1.Tg) mouse model. MUC1.Tg mice express the human MUC1 transgene in normal organs, for example, lung, pancreas, kidneys and other epithelial tissues, in a pattern and at levels consistent with that in humans.[20] MUC1.Tg mice are thus tolerant to MUC1, providing an

experimental setting for the engraftment of LLC/MUC1 cells.[21] MUC1.Tg mice with established LLC/MUC1 tumors were treated with GO-203/NPs to assess the effects of targeting MUC1-C on the tumor microenvironment. GO-203/NP treatment was associated with inhibition of LLC/MUC1 tumor growth as compared with that obtained with empty NPs (Fig. 2A). Analysis of the tumors on day 10 showed that targeting MUC1-C results in downregulation of MUC1 and PD-L1 mRNA levels with increases in IFN-γ expression (Fig. 2B). In addition, targeting MUC1-C resulted in the suppression of PD-L1 protein (Fig. 2C). In concert with our *in vitro* studies, analysis of LLC/MUC1 tumor cells by flow cytometry further demonstrated that targeting MUC1-C decreases PD-L1 expression (Fig. 2D, left and right). We also found that the expression levels of PD-L1 on tumor cells and Ki67 on T-cells were inversely correlated, suggesting that targeting MUC1-C decreases PD-L1 expression on tumors concomitant with a higher proliferative capacity of T-cells surrounding the tumor (Fig. 2E). Consistent with these results, *ex-vivo* analysis of TILs from the GO-203/NP-treated mice

revealed that the CD69 activation marker is upregulated on CD8+ T-cells (Fig. 2F), supporting the notion that targeting MUC1-C activates this population.

Based on these intriguing observations, we performed a more detailed characterization of CD8+ T-cells in the tumor microenvironment. In this way, we found that GO-203/NP treatment is associated with a (i) significant decrease in percentage of CD4+Foxp3+ Tregs (Fig. 3A, left), and (ii) increase in the ratio of CD8+ T-cells to CD4+Foxp3+ Tregs (Fig. 3A, right). Moreover, and consistent with the GO-203/NP-induced upregulation of CD69, *in vitro* stimulation assays revealed that tumor-infiltrating CD8+ T-cells from GO-203/NP-treated mice exhibit increases in expression of IFN-γ (Fig. 3B, left and right), the degranulation marker CD107α (Fig. 3C, left and right), and granzyme B (Fig. 3D). In support of these findings indicative of enhanced function, T-cells from the GO-203/NP-, but not empty NP-, treated mice were highly effective in killing LLC/MUC1 tumor cells (Fig. 3E). These findings support the premise that targeting MUC1-C in LLC/MUC1 tumor cells with the suppression of PD-L1 is effective in restoring and potentiating tumor-infiltrating T-cell function.

Analysis of gene expression data sets showed that MUC1 is expressed at increased levels in NSCLCs compared with that in normal tissue (Fig. 4A) and that MUC1 expression negatively correlates with CD8 (Fig. 4B; R = -0.21, p = 0.0009). We also found that *MUC1* expression negatively correlates with that of *IFNG* (Fig. 4C; R = -0.16, p = 0.015) and *GZMB* (Fig. 4D; R = -0.25, p < 0.0001), indicating that MUC1 suppresses the presence of activated CD8+ TILs in the NSCLC tumor microenvironment. Notably, lower levels of (i) CD8 (Fig. 4E; HR = 0.46, p = 0.041) and (ii) IFNG (Fig. 4F; HR = 0.37, p = 0.0083) expression in NSCLCs were associated with significant decreases in overall survival. These findings in NSCLCs thus lend further support to those obtained in LLC tumors, indicating that MUC1 plays a role in promoting immune evasion.

Aberrant overexpression of MUC1, and specifically the oncogenic MUC1-C subunit, by cancer cells has been linked
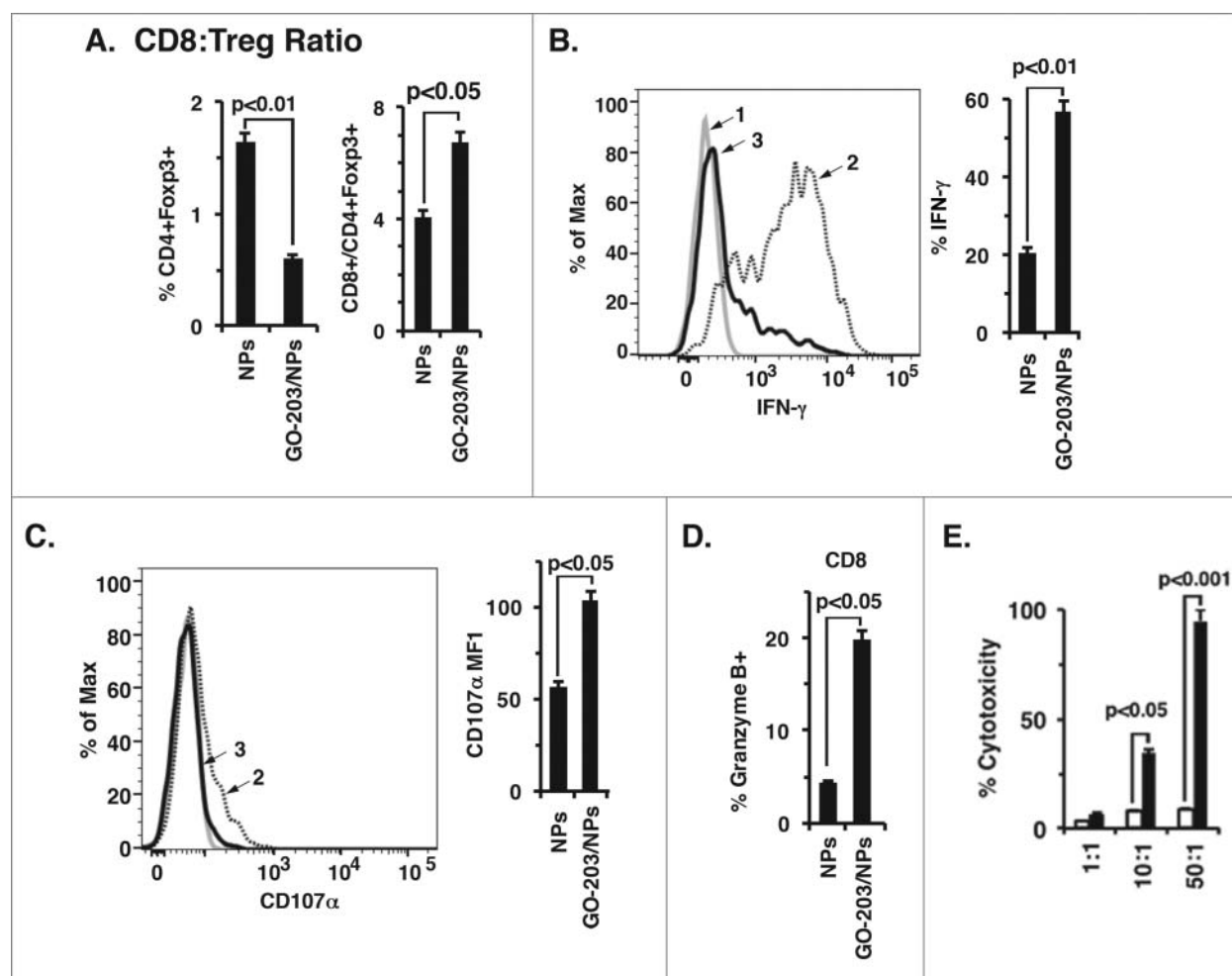

Figure 3. Functional evaluation of TILs from LLC/MUC1 tumors. (A-E) Immune cells were isolated from LLC/MUC1 tumors and then stimulated *ex vivo* for 6 h. (A) The CD45+CD3+ tumor-infiltrating population was analyzed for CD8+ T-cells and CD4+Foxp3+ Tregs. The results (mean ± SD for 4 tumors per group) are expressed as the percentage CD4+Foxp3+ cells (left) and the CD8+/CD4+Foxp3+ ratio (right). (B) Representative histogram depicting IFN-γ production by CD8+ T-cells from NP-treated (profile #3) and GO-203/NP-treated (profile #2) LLC/MUC1 tumors (left). An isotype identical antibody was used as an internal control (profile #1) (left). The results are expressed as the percentage (mean ± SEM for 5 tumors per group) of IFN-γ+ cells (right). (C) Representative histogram showing CD107α expression by CD8+ T-cells from NP-treated (profile #3) and GO-203/NP-treated (profile #2) LLC/MUC1 tumors (left). The results are expressed as the mean fluorescent intensity (MFI; mean ± SEM of 5 tumors per group)(right). (D) CD8+ T-cells were analyzed for granzyme B secretion. The results are expressed as the percentage (mean ± SEM for 5 tumors per group) of granzyme B positive cells. (E) Lymph nodes obtained from NP- and GO-203/NP-treated mice were incubated with LLC/MUC1 target cells at the indicated ratios. The results are expressed as percentage cytotoxicity (mean ± SEM for 5 mice per group) comparing NP-treated mice (open bars) with GO-203/NP-treated mice (solid bars).
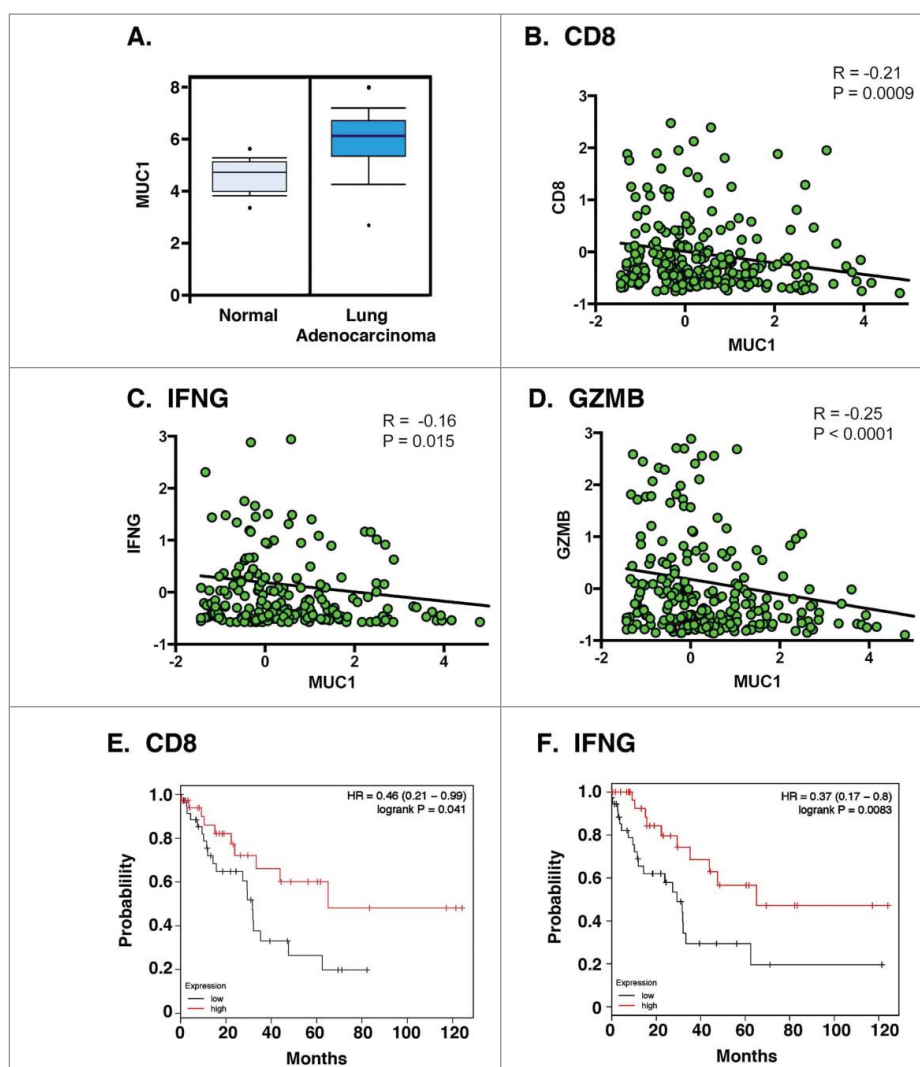
Figure 4. Overexpression of *MUC1* in NSCLC negatively correlates with *CD8, IFNG* and *granzyme (B)(GZMB)*. (A) Microarray data from Oncomine database are expressed as box plots (25th-75th percentiles) for MUC1 expression in normal lung tissues (n = 20) and lung adenocarcinoma (n = 226). The data were log2 transformed and median centered. (B-D) RNA sequencing data of lung cancer patients was obtained from cBioPortal TCGA data set. Correlations between *MUC1* expression and that for *CD8* (B), *IFNG* (C) and *GZMB* (D) were assessed using Spearman's rank correlation coefficient, where *p* < 0.05 was considered as statistically significant. (E-F). Expression of CD8 and IFNG in NSCLC correlates with survival. Kaplan–Meier plots comparing the overall survival of patients with NSCLC in the TCGA data set. Patients were stratified with the high (red) or low (blue) expression of *CD8* (E) and *IFNG* (F) against the median average. The survival curves were compared using log-rank (Mantel–Cox) test. HR, hazard ratio.

with protection from killing by (i) TRAIL, (ii) Fas ligand, and (iii) T-cell perforin/granzyme B-mediated lysis.[22,23] The demonstration that MUC1-C induces PD-L1 and suppresses IFN-γ in NSCLC cells has further supported the notion that this oncoprotein integrates a program of EMT and immune evasion.[13,14] The present studies provide the first evidence that MUC1-C drives the dysregulation of PD-L1 and IFN-γ in the tumor microenvironment and that targeting MUC1-C induces cytotoxic TILs against the tumor. Notably, targeting MUC1-C with GO-203/NPs in the MUC1.Tg model had no apparent adverse effects, such as weight loss or other overt toxicity, indicating that MUC1-C is a potential target for reprogramming of the suppressive tumor microenvironment with induction of antitumor immunity. In this respect and regarding translational relevance, a Phase I trial of GO-203 in patients with advanced solid tumors demonstrated an acceptable safety profile and clinical activity. The formulation of GO-203 in NPs[19] is now being advanced for more sustained and less frequent dosing of

patients with NSCLC and other malignancies in Phase I-II studies. Based on the present findings, trials with the GO-203/NPs will be integrated with the administration of immune checkpoint inhibitors or other immunotherapeutic approaches.

Materials and methods

Cell culture

Mouse LLC cells stably transfected with full length MUC1 (gift from Dr. Stephen Tomlinson, Medical University of South Carolina, Charleston, SC) were grown in DMEM medium supplemented with 10% heat-inactivated fetal bovine serum (HI-FBS), 100μg/ml streptomycin, 100 units/ml penicillin and 2 mM L-glutamine. LLC cells were transfected with lentiviral vectors to stably express a control vector or MUC1-C. Geneticin (LLC/MUC1) and hygromycin (LLC/Vector, LLC/MUC1-C) were used to maintain a selection pressure. Authentication

of the cells was performed by short tandem repeat (STR) analysis. Mycoplasma levels were measured monthly using the MycoAlert Mycoplasma Detection Kit (Lonza, Rockland, MA, USA).

Immunoblot analysis

Whole cell lysates were prepared in NP-40 lysis buffer and immunoblotted with (i) anti-MUC1-C (ThermoFisher Scientific, Waltham, MA, USA; Cat. #HM-1630-P1) and an anti-Armenian hamster secondary antibody (Abcam, Cambridge, MA, USA; Cat. #ab5745), (ii) anti-PD-L1 (R&D Systems, Minneapolis, MN, USA; Cat. #AF1019) and an anti-goat secondary antibody (Santa Cruz Biotechnology, Dallas, TX, USA; Cat. #SC-2028, 1:3000 dilution) and (iii) anti-β-actin (Sigma, St. Louis, MO, USA; Cat. A5316) and an anti-mouse secondary antibody (GE Healthcare Life Sciences, Pittsburgh, PA, USA; Cat. #NA931). Horseradish peroxidase secondary antibodies and enhanced chemiluminescence (GE Healthcare Life Sciences) were used for the detection of immune complexes. Immunoblot results were each confirmed with 2 other analysis.

Quantitative real-time, reverse transcriptase PCR (qRT-PCR)

The RNeasy mini kit (Qiagen, Germantown, MD, USA) was used to isolate whole cell RNA. The High Capacity cDNA Reverse Transcription kit (Life Technologies, Carlsbad, CA, USA) was used to synthesize cDNAs from 2 μg RNA. The GAPDH gene was used as an internal control. The SYBR green qPCR assay kit and the ABI Prism Sequence Detector (Applied Biosystems, Foster City, CA, USA) were used to amplify the cDNAs.

Animal studies

LLC/MUC1 cells (10^6 cells) were injected subcutaneously in the flank of 6-week old MUC1.Tg mice. The mice were grouped and treated with control NPs or 15 mg/kg GO-203/NPs once a week for 2 weeks. At the end of the treatment, tumor tissues were harvested and processed for multi-parameter staining. These studies were performed under animal protocol #12–029 approved by the DFCI Animal Use and Care Committee.

Flow cytometry

To generate cell suspensions, tumors were cut into small pieces, and further dissociated in RPMI-1640 buffer containing 5% FBS, 100 IU/ml collagenase type IV (Invitrogen, Carlsbad, CA, USA), and 50 μg/ml DNAse I (Roche, Basel, Switzerland) for 45 min at 37° C. After incubation, cells were treated with red blood cell lysis buffer and filtered through a 70 μm cell strainer. After centrifugation, cell pellets were resuspended in 1xPBS/2% FBS. Approximately 0.5–1 $\times$ 10^6 cells were stained for surface markers in 1xPBS/2% FBS for 15 min at 4°C. Intracellular staining was performed for granzyme B using the Foxp3 staining buffer set (eBioscience, Santa Clara, CA, USA). For intracellular cytokine detection assays, immune cells from tumors were

obtained after Ficoll gradient separation. Cells (1 $\times$ 10^6) were cultured with PMA (50 ng) and ionomycin (500 ng) for 6 h at 37° C. GolgiPlug (BD PharMingen, San Jose, CA, USA) and FITC-conjugated CD107α (Biolegend, San Diego, CA, USA; 1D4B) were added for the last 5 h of culture. The Cytofix/Cytoperm kit (BD Biosciences, San Jose, CA) was used for intracellular cytokine staining. Briefly, cells were washed with 1x PBS after harvesting, then stained for surface markers including CD8, and CD3, followed by intracellular staining with PE-conjugated anti-IFN-γ, and Pacific blue anti-granzyme B or respective isotype-matched mAbs. In all stained samples, dead cells were excluded using Live/Dead Fixable Dead Cell staining kit (Invitrogen). Cells were acquired on the LSR Fortessa (BD Biosciences) and analyzed with FlowJo software (Tree Star, Ashland, OR, USA).

The following antibodies were used for staining in FACS analyses: FITC/AF488-conjugated mAbs to CD45(30-F11), PE-conjugated mAbs to IFN-γ (XMG1.2), PerCP-conjugated mAbs to Nkp46(29A1.4), CD45(30-F11), APC/AF647-conjugated mAbs to PD-L1(10F.9G2), Foxp3(FJK-16s), Rat IgG (eBR2a), Pacific Blue/BV421-conjugated mAbs to Ki67(16A8), granzyme B(GB11), CD4(RM4–5), Rat IgG(eBRG1), PE-Cy7-conjugated mAbs to CD3(17A2), CD62L(MEL-14), PD-L1 (10F.9G2), CD69(H1.2F3), Rat IgG(RTK2758), APC-Cy7-conjugated mAbs to CD4(GK1.5), Alexa-Fluor 700-conjugated mAbs to CD8(53–6.7), Rat IgG(RTK4530), were purchased from BD Biosciences, Biolegend or eBioscience.

CTL assays

The day before mice sacrifice, LLC/MUC1 cells (6 $\times$ 10^3 per well) were plated in 96-well plates and incubated overnight. Lymph nodes were harvested, digested with ACK lysis buffer (GIBCO, Waltham, MA, USA) and rinsed with PBS. Cells (effector cells) were incubated with LLC/MUC1 cells (target cells) at different ratios in 96 well-plates for 6 h. The percentage of cytotoxicity was determined by measuring LDH release following the manufacturer's recommendations (CytoTox 96® Non-Radioactive Cytotoxicity Assay; Promega, Madison, WI, USA) and calculated using the formula: (Experimental-Effector spontaneous-Target spontaneous)/(Target maximum-Target spontaneous) x 100.

Bioinformatic analysis

Clinical data of NSCLC patients was obtained from cBioPortal TCGA data sets [24]. Correlations between *MUC1* and *CD8* (*CD8A/B*), *IFNG* and *GZMB* expression were assessed using Spearman's coefficient. The prognostic value of CD8 and IFNG in NSCLC patients was performed as described.[25] Multiple probe set IDs were averaged for each sample. Patients were divided by the median expression. The Kaplan–Meier survival probability plot with the hazard ratio (95% confidence interval) and log-rank P-value were calculated and plotted in R.

Statistical analysis

Normal distribution of the data was confirmed using the Shapiro-Wilk test. The Student's t-test was used to determine

statistical significance (GraphPad Software Inc., LaJolla, CA, USA).

References

1. Borghaei H, Paz-Ares L, Horn L, Spigel DR, Steins M, Ready NE, Chow LQ, Vokes EE, Felip E, Holgado E, et al. Nivolumab versus docetaxel in advanced nonsquamous non-small-cell lung cancer. N Engl J Med 2015; 373:1627-39; PMID:26412456; https://doi.org/10.1056/NEJMoa1507643

2. Brahmer J, Reckamp KL, Baas P, Crino L, Eberhardt WE, Poddubskaya E, Antonia S, Pluzanski A, Vokes EE, Holgado E, et al. Nivolumab versus docetaxel in advanced squamous-cell non-small-cell lung cancer. N Engl J Med 2015; 373:123-35; PMID:26028407; https://doi.org/10.1056/NEJMoa1504627

3. Gettinger SN, Horn L, Gandhi L, Spigel DR, Antonia SJ, Rizvi NA, Powderly JD, Heist RS, Carvajal RD, Jackman DM, et al. Overall survival and long-term safety of Nivolumab (Anti-Programmed Death 1 Antibody, BMS-936558, ONO-4538) in patients with previously treated advanced non-small-cell lung cancer. J Clin Oncol 2015; 33:2004-12; PMID:25897158; https://doi.org/10.1200/JCO.2014.58.3708

4. Herbst RS, Baas P, Kim DW, Felip E, Perez-Gracia JL, Han JY, Molina J, Kim JH, Arvis CD, Ahn MJ, et al. Pembrolizumab versus docetaxel for previously treated, PD-L1-positive, advanced non-small-cell lung cancer (KEYNOTE-010): a randomised controlled trial. Lancet 2016; 387:1540-50; PMID:26712084; https://doi.org/10.1016/S0140-6736(15)01281-7

5. Fehrenbacher L, Spira A, Ballinger M, Kowanetz M, Vansteenkiste J, Mazieres J, Park K, Smith D, Artal-Cortes A, Lewanski C, et al. Atezolizumab versus docetaxel for patients with previously treated non-small-cell lung cancer (POPLAR): a multicentre, open-label, phase 2 randomised controlled trial. Lancet 2016; 387:1837-46; PMID:26970723; https://doi.org/10.1016/S0140-6736(16)00587-0

6. Carrizosa DR, Gold KA. New strategies in immunotherapy for non-small cell lung cancer. Transl Lung Cancer Res 2015; 4:553-9; PMID:26629424; https://doi.org/10.3978/j.issn.2218-6751.2015.06.05

7. Donnem T, Hald SM, Paulsen EE, Richardsen E, Al-Saad S, Kilvaer TK, Brustugun OT, Helland A, Lund-Iversen M, Poehl M, et al. Stromal CD8+ T-cell Density-a promising supplement to TNM staging in non-small cell lung cancer. Clin Cancer Res 2015; 21:2635-43; PMID:25680376; https://doi.org/10.1158/1078-0432.CCR-14-1905

8. Bremnes RM, Busund LT, Kilvaer TL, Andersen S, Richardsen E, Paulsen EE, Hald S, Khanehkenari MR, Cooper WA, Kao SC, et al. The role of tumor-infiltrating lymphocytes in development, progression, and prognosis of non-small cell lung cancer. J Thorac Oncol 2016; 11:789-800; PMID:26845192; https://doi.org/10.1016/j.jtho.2016.01.015

9. Tokito T, Azuma K, Kawahara A, Ishii H, Yamada K, Matsuo N, Kinoshita T, Mizukami N, Ono H, Kage M, et al. Predictive relevance of PD-L1 expression combined with CD8+ TIL density in stage III non-small cell lung cancer patients receiving concurrent chemoradiotherapy. Eur J Cancer 2016; 55:7-14; PMID:26771872; https://doi.org/10.1016/j.ejca.2015.11.020

10. Situ D, Wang J, Ma Y, Zhu Z, Hu Y, Long H, Rong T. Expression and prognostic relevance of MUC1 in stage IB non-small cell lung cancer. Med Oncol 2010; 28:596-604; PMID:21116877; https://doi.org/10.1007/s12032-010-9752-4

11. Khodarev N, Pitroda S, Beckett M, MacDermed D, Huang L, Kufe D and Weichselbaum R. MUC1-induced transcriptional programs associated with tumorigenesis predict outcome in breast and lung cancer. Cancer Res 2009; 69:2833-7; PMID:19318547; https://doi.org/10.1158/0008-5472.CAN-08-4513

12. Xu F, Liu F, Zhao H, An G and Feng G. Prognostic significance of mucin antigen MUC1 in various human epithelial cancers: a meta-analysis. Medicine (Baltimore) 2015; 94:e2286; PMID:26683959; https://doi.org/10.1097/MD.0000000000002286

13. Rajabi H, Kufe D. MUC1-C oncoprotein integrates a program of EMT, epigenetic reprogramming and immune evasion in human carcinomas. BBA Rev Cancer 2017; 1868:117-22; PMID:28302417; https://doi.org/10.1016/j.bbcan.2017.03.003

14. Bouillez A, Rajabi H, Jin C, Samur M, Tagde A, Alam M, Hiraki M, Maeda T, Hu X, Adeegbe D, et al. MUC1-C integrates PD-L1 induction with repression of immune effectors in non-small cell lung cancer. Oncogene 2017 Mar 13 [Epub ahead of print]; https://doi.org/10.1038/onc.2017.47

15. Kufe D. Mucins in cancer: function, prognosis and therapy. Nat Rev Cancer 2009; 9:874-85; PMID:19935676; https://doi.org/10.1038/nrc2761

16. Kufe D. MUC1-C oncoprotein as a target in breast cancer: activation of signaling pathways and therapeutic approaches. Oncogene 2013; 32:1073-81; PMID:22580612; https://doi.org/10.1038/onc.2012.158

17. Raina D, Kosugi M, Ahmad R, Panchamoorthy G, Rajabi H, Alam M, Shimamura T, Shapiro G, Supko J, Kharbanda S, et al. Dependence on the MUC1-C oncoprotein in non-small cell lung cancer cells. Mol Cancer Ther 2011; 10:806-16; PMID:21421804; https://doi.org/10.1158/1535-7163.MCT-10-1050

18. Raina D, Ahmad R, Rajabi H, Panchamoorthy G, Kharbanda S, Kufe D. Targeting cysteine-mediated dimerization of the MUC1-C oncoprotein in human cancer cells. Int J Oncol 2012; 40:1643-9; PMID:22200620; https://doi.org/10.3892/ijo.2011.1308

19. Hasegawa M, Sinha RK, Kumar M, Alam M, Yin L, Raina D, Kharbanda A, Panchamoorthy G, Gupta D, Singh H, et al. Intracellular targeting of the oncogenic MUC1-C protein with a novel GO-203 nanoparticle formulation. Clin Cancer Res 2015; 21:2338-47; PMID:25712682; https://doi.org/10.1158/1078-0432.CCR-14-3000

20. Rowse GJ, Tempero RM, VanLith ML, Hollingsworth MA, Gendler SJ. Tolerance and immunity to MUC1 in a human MUC1 transgenic murine model. Cancer Res 1998; 58:315-21; PMID:9443411

21. Gong J, Chen D, Kashiwaba M, Li Y, Takeuchi H, Qu H, Rowse GJ, Gendler SJ, Kufe DW. Reversal of tolerance to human MUC1 antigen in MUC1 transgenic mice immunized with fusions of dendritic and carcinoma cells. Proc Natl Acad Sci USA 1998; 95:6279-83; PMID:9600956; https://doi.org/10.1073/pnas.95.11.6279

22. Agata N, Kawano T, Ahmad R, Raina D, Kharbanda S, Kufe D. MUC1 oncoprotein blocks death receptor-mediated apoptosis by inhibiting recruitment of caspase-8. Cancer Res 2008; 68:6136-44; PMID:18676836; https://doi.org/10.1158/0008-5472.CAN-08-0464

23. David JM, Hamilton DH, Palena C. MUC1 upregulation promotes immune resistance in tumor cells undergoing brachyury-mediated epithelial-mesenchymal transition. Oncoimmunology 2016; 5:e1117738; PMID:27141403; https://doi.org/10.1080/2162402X.2015.1117738

24. Gao J, Aksoy BA, Dogrusoz U, Dresdner G, Gross B, Sumer SO, Sun Y, Jacobsen A, Sinha R, Larsson E, et al. Integrative analysis of complex cancer genomics and clinical profiles using the cBioPortal. Sci Signal 2013; 6:pl1; PMID:23550210; https://doi.org/10.1126/scisignal.2004088

25. Gyorffy B, Surowiak P, Budczies J, Lanczky A. Online survival analysis software to assess the prognostic value of biomarkers using transcriptomic data in non-small-cell lung cancer. PLoS One 2013; 8:e82241; PMID:24367507; https://doi.org/10.1371/journal.pone.0082241